

Rectifying the Optical-Field-Induced Current in Dielectrics: Petahertz Diode

J. D. Lee,^{1,*} Won Seok Yun,¹ and Noejung Park²

¹*Department of Emerging Materials Science, DGIST, Daegu 711-873, Korea*

²*School of Natural Science and Low-Dimensional Carbon Materials Center, UNIST, Ulsan 689-798, Korea*

(Received 24 July 2015; published 3 February 2016)

Investigating a theoretical model of the optical-field-induced current in dielectrics driven by strong few-cycle laser pulses, we propose an asymmetric conducting of the current by forming a heterojunction made of two distinct dielectrics with a low hole mass ($m_h^* \ll m_e^*$) and low electron mass ($m_e^* \ll m_h^*$), respectively. This proposition introduces the novel concept of a petahertz (10^{15} Hz) diode to rectify the current in the petahertz domain, which should be a key ingredient for the electric signal manipulation of future light-wave electronics. Further, we suggest the candidate dielectrics for the heterojunction.

DOI: [10.1103/PhysRevLett.116.057401](https://doi.org/10.1103/PhysRevLett.116.057401)

High-intensity subfemtosecond laser sources with waveform controllability have opened up a new horizon to the nonlinear and extreme ultrafast dynamics of matter [1]. For instance, single attosecond ($1 \text{ as} = 10^{-18} \text{ s}$) pulses in the extreme ultraviolet (XUV) frequency range have allowed new time-domain insight into the fundamental electronic processes in atoms, molecules, and solids at the time scale of 10–1000 as [1–12]. Among those, subfemtosecond electronic processes in the solid state are found particularly interesting because of their potential relevance to petahertz (10^{15} Hz) signal processing [4,10–12].

Recently, Schiffrin *et al.* [13] have demonstrated that a strong few-cycle optical waveform induces the macroscopic charge separation and electric current in SiO_2 , a large band-gap dielectric. Although the observations of optically controlled currents have been reported in the diverse nanostructures [14–16], this finding is remarkable in that the reversible and robust transient current is driven in the bulk solid state below the optical breakdown threshold. This picture of optical-field-induced currents in dielectrics or wide band-gap semiconductors has been studied based on the independent particle models [17,18]. In addition to that, the adiabatic and reversible band response has been discussed in a limit of the strong field intensity [19]. Further, very recently Wachter *et al.* [20] investigated the nonlinear generation of the optical-field-induced currents in the bulk insulators in terms of the first-principles simulation of the time-dependent density functional theory (TDDFT).

One of the open questions may be whether the optical-field-induced current could be directly accessible to the signal processing. In modern electronics based on semiconductor technology, the diode made of a heterojunction with the p -type and n -type semiconductors plays the most fundamental role for the purpose [21]. In sharp contrast to the p -type or n -type semiconductors (where holes or electrons are chemically doped, respectively), however, the optical pumping (or optical doping) creates holes and

electrons simultaneously in the dielectrics, both of which could participate in inducing and carrying the current.

In this Letter, we devise an asymmetric conduction to rectify the optical-field-induced current in dielectrics under the optical pumping by strong few-cycle laser pulses. A theoretical model of the heterojunction is suggested, which is composed of two different dielectrics with a low hole mass ($m_h^* \ll m_e^*$) and low electron mass ($m_e^* \ll m_h^*$), respectively. We find that the tunneling current across the junction flows along one direction from the low-hole-mass dielectric to low-electron-mass one. This finding constitutes the petahertz diode, which should possibly pave the way for petahertz signal processing of light-wave electronics in the future. We also advise the candidate dielectrics for forming the desired heterojunction.

We start with a standard tight-binding Hamiltonian \mathcal{H}_m describing the band electrons in a dielectric. It is combined with the optical pumping $\mathcal{H}'(\tau)$ by the linearly polarized optical field $\mathbf{A}(\tau)$, which makes the problem effectively one dimensional; i.e., the crystallographic planes stacked say along the field polarization ($\propto \hat{\mathbf{z}}$) define the lattice sites. Thus, we have $\mathcal{H}_0 = \mathcal{H}_m + \mathcal{H}'(\tau)$,

$$\begin{aligned} \mathcal{H}_m &= \varepsilon_c \sum_l c_l^\dagger c_l + \varepsilon_v \sum_l d_l^\dagger d_l \\ &+ \frac{\Delta_c}{4} \sum_l (c_l^\dagger c_{l+1} + \text{H.c.}) + \frac{\Delta_v}{4} \sum_l (d_l^\dagger d_{l+1} + \text{H.c.}), \\ \mathcal{H}'(\tau) &= A(\tau) j_c + A(\tau) j_v + A(\tau) \bar{d} \sum_l (c_l^\dagger d_l^\dagger + \text{H.c.}), \end{aligned} \quad (1)$$

where c_l^\dagger (c_l) and d_l^\dagger (d_l) are the electron and hole operators with the energy levels ε_c and ε_v at the lattice site l , respectively, and Δ_c and Δ_v are their hopping parameters. Indices of c and v mean the conduction and valence bands. The few-cycle optical field $\mathbf{A}(\tau)$, i.e., $\mathbf{A}(\tau) = A_0 \exp(-\tau^2/\bar{\tau}^2) \cos(\omega\tau + \phi) \hat{\mathbf{z}} = -A(\tau) \hat{\mathbf{z}}$ and hence $\mathbf{E}(\tau) = \partial/\partial\tau A(\tau) \hat{\mathbf{z}}$, with the carrier envelop phase ϕ [22] is assumed. The intraband transitions are given by the current operators

$j_c = it_c \sum_l (c_l^\dagger c_{l+1} - c_{l+1}^\dagger c_l)$ and $j_v = -it_v \sum_l (d_l^\dagger d_{l+1} - d_{l+1}^\dagger d_l)$ with $t_{c(v)} = \int dz u_{c(v);l}^*(z) p_z u_{c(v);l+1}(z)$ and the interband transition by $\bar{d} = \int dz u_{c;l}^*(z) p_z u_{v;l}(z)$. $u_{c(v);l}(z)$ is the l -centered localized orbital. If we express the Hamiltonian \mathcal{H} in the k space, the band features become transparent:

$$\begin{aligned} \mathcal{H}_0 = & \sum_k E_k^c(\tau) c_k^\dagger c_k + \sum_k E_{-k}^v(\tau) d_{-k}^\dagger d_{-k} \\ & + A(\tau) \bar{d} \sum_k (c_k^\dagger d_{-k}^\dagger + d_{-k} c_k), \end{aligned} \quad (2)$$

where $E_k^c(\tau)$ and $E_{-k}^v(\tau)$ are the effective electron and hole energies given by $E_k^c(\tau) = \varepsilon_k^c - t_c A(\tau) \sin(ka)$ and $E_{-k}^v(\tau) = \varepsilon_{-k}^v - t_v A(\tau) \sin(ka)$ with the lattice constant a . ε_k^c and ε_{-k}^v are the tight-binding bands, $\varepsilon_k^c = \varepsilon_c + (\Delta_c/2) \cos(ka)$ and $\varepsilon_{-k}^v = \varepsilon_v + (\Delta_v/2) \cos(ka)$.

Turning on the strong optical field $\mathbf{A}(\tau)$, for which $\bar{\tau} = 4$ fs and $\omega = 1.7$ eV will be used hereafter unless mentioned otherwise, electrons and holes are excited and the relevant dynamics are initiated. Such dynamics can be described by the time-dependent Schrödinger equation $i(\partial/\partial\tau)|\Psi(\tau)\rangle = \mathcal{H}_0|\Psi(\tau)\rangle$,

$$|\Psi(\tau)\rangle = C(\tau)|0,0\rangle + \sum_k C(k,\tau)|k,-k\rangle \quad (3)$$

with $|\Psi(0)\rangle = |0,0\rangle$. We here simplified the notation as $|a,b\rangle = |a\rangle_c |b\rangle_v$, that is, $|k\rangle_c = c_k^\dagger |0\rangle_c$ and $|k\rangle_v = d_k^\dagger |0\rangle_v$. From the solution of the time-dependent Schrödinger equation, we calculate the optical-field-induced current $J(\tau)$, i.e., $J(\tau) = \langle \Psi(\tau) | (j_c + j_v) | \Psi(\tau) \rangle = \sum_k [t_c \sin(ka) + t_v \sin(ka)] |C(k,\tau)|^2$.

In Figs. 1(a) and 1(b), we provide the results of $J(\tau)$ in a dielectric with an energy gap $E_g = 8$ eV (e.g., for SiO₂) at $\phi = 0$ and $\pi/2$. With this, the light-matter interaction is reversible in the adiabatic limit ($\omega \ll E_g$) [19] and the experimental observation of the current [13] is reproduced. As illustrated in Fig. 1(c), in terms of $E_k^c(\tau)$ and $-E_{-k}^v(\tau)$, the displacements of the conduction and valence bands are caused, which makes the population unbalanced between $k > 0$ and $k < 0$ and eventually drives the current. Total charge transfer Q in Fig. 1(d) is calculated by $Q = \int_{-\infty}^{\infty} d\tau J(\tau)$. This is consistent with an actual measurement in the principle experiment [13].

Now we extend our consideration to an interesting heterojunction composed of two distinct dielectrics. Figure 2(a) displays that the heterojunction in our consideration should consist of a dielectric with the low hole mass ($m_h^* \ll m_e^*$) in the left side and the other with the low electron mass ($m_e^* \ll m_h^*$) in the right side. One may then expect the shifts of the effective conduction and valence bands of dielectrics depending on $A(\tau) > 0$ and $A(\tau) < 0$ as shown in Fig. 2(b). We aim to examine the tunneling

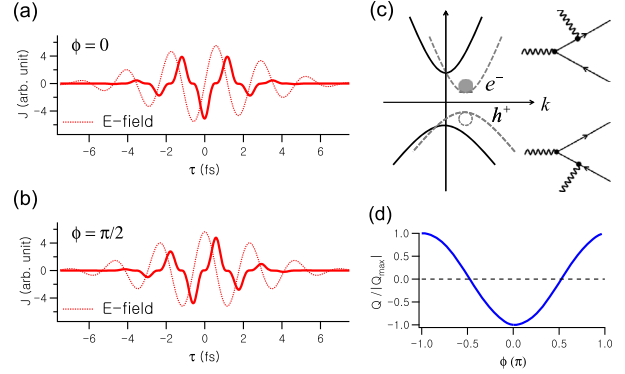


FIG. 1. (a),(b) Optical-field-induced current at $\phi = 0$ and $\pi/2$. Necessary parameters are taken as follows: $\varepsilon_c = 5$ eV, $\Delta_c = -3$ eV, $\varepsilon_v = 5$ eV, $\Delta_v = -1$ eV, $t_c/\omega = 1.76$ Å, $t_v/\omega = 0.59$ Å, $\bar{d}/\omega = 1.6$ Å, and $E_0 = A_0\omega = 0.43$ V/Å. (c) Displacements of the effective conduction and valence bands $E_k^c(\tau)$ and $-E_{-k}^v(\tau)$ at an instant of $A(\tau) > 0$ (gray dashed bands). Black solid bands are at $A(\tau) = 0$. Feynman diagrams describe the physical processes of creation of the optical-field-induced current, where the wavy line denotes the optical field. e^- (shaded ball) and h^+ (empty ball) represent the photoexcited electron and hole, respectively. (d) Total charge transfer Q with respect to ϕ .

current across the heterojunction under the high intensity optical pumping in the same way as the previous homogeneous dielectric.

To explore the tunneling problem across the heterojunction of Fig. 2(a), we now consider an extended Hamiltonian \mathcal{H}

$$\mathcal{H} = \mathcal{H}_L + \mathcal{H}_R + \mathcal{H}_T, \quad (4)$$

where \mathcal{H}_L and \mathcal{H}_R are corresponding to \mathcal{H}_0 of Eq. (2) for the dielectrics in the left (L) and right (R) sides, respectively, and the tunneling term \mathcal{H}_T across the junction

$$\begin{aligned} \mathcal{H}_T = & \lambda T_{cc} \sum_{kk'} (c_{L:k}^\dagger c_{R:k'} + c_{R:k}^\dagger c_{L:k'}) \\ & + \lambda T_{vv} \sum_{kk'} (d_{R:k}^\dagger d_{L:k'} + d_{L:k}^\dagger d_{R:k'}) \\ & + \lambda T_{cv} \sum_{kk'} (c_{L:k}^\dagger d_{R:k'}^\dagger + d_{R:k} c_{L:k'}) \\ & + \lambda T_{vc} \sum_{kk'} (c_{R:k} d_{L:k'} + d_{L:k}^\dagger c_{R:k'}^\dagger). \end{aligned} \quad (5)$$

$c_{L(R):k}^\dagger$ or $c_{L(R):k}$ and $d_{L(R):k}^\dagger$ or $d_{L(R):k}$ are electron and hole operators in the dielectric of the left (right) side of the junction. T_{cc} , T_{vv} , T_{cv} , and T_{vc} are the tunneling matrices and λ is a controlling parameter. Dynamics of the heterojunction under the optical pumping can be also described by the time-dependent Schrödinger equation $i(\partial/\partial\tau)|\Psi(\tau)\rangle = \mathcal{H}|\Psi(\tau)\rangle$. $|\Psi(\tau)\rangle$ is now written as

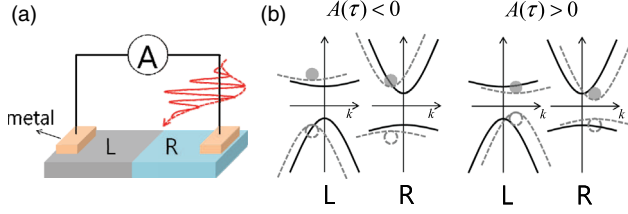


FIG. 2. (a) Heterojunction made of two different dielectrics in the left (L) and right (R) sides. (b) A dielectric with the low hole mass ($m_h^* \ll m_e^*$) is assumed to be in the left side and the other with the low electron mass ($m_e^* \ll m_h^*$) in the right side. Effective conduction and valence bands shift according to an oscillation of the optical field.

$$\begin{aligned}
 |\Psi(\tau)\rangle &= C(\tau)|0,0\rangle_L|0,0\rangle_R \\
 &+ \sum_k C_k^L(\tau)|k,-k\rangle_L|0,0\rangle_R \\
 &+ \sum_k C_k^R(\tau)|0,0\rangle_L|k,-k\rangle_R \\
 &+ \sum_{kk'} C_{kk'}^{LR}(\tau)|k,-k\rangle_L|k',-k'\rangle_R \\
 &+ \sum_{kk'} D_{kk'}^{cc}(\tau)|k,0\rangle_L|k',0\rangle_R \\
 &+ \sum_{kk'} D_{kk'}^{cv}(\tau)|k,0\rangle_L|0,k'\rangle_R \\
 &+ \sum_{kk'} D_{kk'}^{vc}(\tau)|0,k\rangle_L|k',0\rangle_R \\
 &+ \sum_{kk'} D_{kk'}^{vv}(\tau)|0,k\rangle_L|0,k'\rangle_R, \quad (6)
 \end{aligned}$$

where $|a,b\rangle_{L(R)}$ stands for $|a\rangle_c|b\rangle_v$ of the left(right)-side dielectric. Solving the time-dependent Schrödinger equation for $|\Psi(\tau)\rangle$, one may evaluate the electron and hole occupations of both left and right sides like $n_{L(R)}^c(\lambda, \tau) = \sum_k \langle \Psi(\tau) | c_{L(R):k}^\dagger c_{L(R):k} | \Psi(\tau) \rangle = \sum_k |C_k^{L(R)}(\tau)|^2 + \sum_{kk'} [|C_{kk'}^{LR}(\tau)|^2 + |D_{kk'}^{cv(vc)}(\tau)|^2]$ and further $n_{L(R)}^v(\lambda, \tau) = \sum_k \langle \Psi(\tau) | d_{L(R):k}^\dagger d_{L(R):k} | \Psi(\tau) \rangle = \sum_k |C_k^{L(R)}(\tau)|^2 + \sum_{kk'} [|C_{kk'}^{LR}(\tau)|^2 + |D_{kk'}^{vc(cv)}(\tau)|^2]$ and obtain, in a limit of $\lambda \rightarrow 0$,

$$\begin{aligned}
 n_{L(R)}^c(\lambda, \tau) &= n_{L(R)}^c(0, \tau) + \lambda^2 \mathcal{N}_{L(R)}^c(\tau) + \dots, \\
 n_{L(R)}^v(\lambda, \tau) &= n_{L(R)}^v(0, \tau) + \lambda^2 \mathcal{N}_{L(R)}^v(\tau) + \dots. \quad (7)
 \end{aligned}$$

At the end of the calculation, putting $\lambda = 1$, we guarantee that $\mathcal{N}_{L(R)}^c(\tau)$ and $\mathcal{N}_{L(R)}^v(\tau)$ should be band occupations relevant to the lowest-order tunneling between two dielectrics. Now the tunneling current $J_T(\tau)$ across the junction can be simply given by [23]

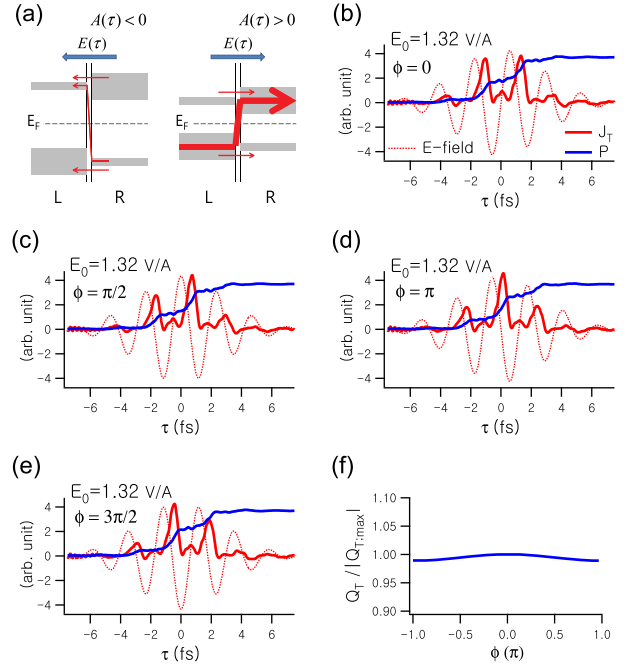


FIG. 3. (a) Schematic drawings of the tunneling conduction across the junction under the strong optical pumping. Gray-colored areas mean the bandwidths and E_F is the Fermi level of the junction. Left panel depicts the worst situation and right panel the best situation for the tunneling conduction. Thickness of red arrows may be understood as the current density. (b)–(e) Tunneling current $J_T(\tau)$ and transferred charge $P(\tau)$ with respect to τ at $\phi = 0, \pi/2, \pi$, and $3\pi/2$ and $E_0 = 1.32 \text{ V/\AA}$. Rectified optical-field-induced currents are obtained. (f) Total transferred (tunneling) charge Q_T with respect to ϕ at $E_0 = 1.32 \text{ V/\AA}$.

$$J_T(\tau) = \frac{\partial}{\partial \tau} P(\tau) = -\frac{\partial}{\partial \tau} [\mathcal{N}_L^c(\tau) - \mathcal{N}_L^v(\tau)], \quad (8)$$

where $P(\tau) = -\mathcal{N}_L^c(\tau) + \mathcal{N}_L^v(\tau) = \mathcal{N}_R^c(\tau) - \mathcal{N}_R^v(\tau)$.

For an actual calculation, we ideally arrange the extreme low-hole-mass dielectric and the extreme low-electron-mass dielectric symmetrically such that the hole band of the former should have the same width as the electron band of the latter, and the converse. We thus have $\varepsilon_{L:k}^c = \varepsilon_L^c + (\Delta_1/2) \cos(ka)$, $\varepsilon_{L:k}^v = \varepsilon_L^v + (\Delta_0/2) \cos(ka)$, $\varepsilon_{R:k}^c = \varepsilon_R^c + (\Delta_0/2) \cos(ka)$, and $\varepsilon_{R:k}^v = \varepsilon_R^v + (\Delta_1/2) \cos(ka)$, where $\varepsilon_L^c = (\Delta - \Delta_0)/2$, $\varepsilon_L^v = \Delta/2$, $\varepsilon_R^c = \Delta/2$, and $\varepsilon_R^v = (\Delta - \Delta_0)/2$ with $\Delta = 8 \text{ eV}$, $\Delta_0 = -6 \text{ eV}$, and $\Delta_1 = -0.5 \text{ eV}$. Thus, hole (electron) and electron (hole) bandwidths of the low-hole(electron)-mass dielectric correspond to $|\Delta_0|$ and $|\Delta_1|$, respectively, and the energy gap is 7.75 eV for both dielectrics. This is schematically illustrated in Fig. 3(a), where the gray-colored areas mean the bandwidths. We also adopt $t_L^c/\omega = 0.3 \text{ \AA}$, $t_L^v/\omega = 3.4 \text{ \AA}$, $t_R^c/\omega = 3.4 \text{ \AA}$, $t_R^v/\omega = 0.3 \text{ \AA}$, and $d_{L(R)}/\omega = 1.5 \text{ \AA}$. For the tunneling, in addition, we adopt $T_{cc} = T_{vv} = 340 \text{ meV}$ and $T_{cv} = T_{vc} = 68 \text{ meV}$, i.e., $T_{cv} \ll T_{cc}$ and $T_{vc} \ll T_{vv}$.

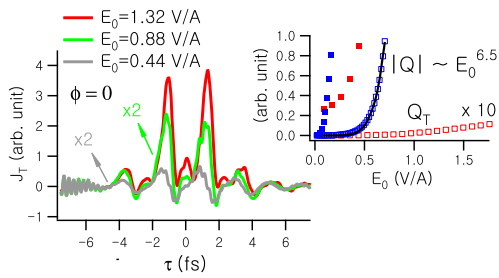


FIG. 4. Tunneling currents $J_T(\tau)$ at the electric field strengths $E_0 = 1.32, 0.88,$ and 0.44 V/Å and $\phi = 0$. Inset shows the behavior of $|Q|$ [for an homogeneous dielectric, i.e., Fig. 1(d); blue empty squares] and Q_T (red empty squares) with respect to the electric field strength E_0 at $\phi = 0$. Blue and red filled squares indicate $|Q| \times 500$ and $Q_T \times 5000$, respectively.

Figure 3(a) shows what happens in the junction made of two dielectrics under the strong optical pumping. It is essential to note that, due to the sharp difference between electron and hole masses (in other words, between electron and hole mobilities), the tunneling transport should occur mainly along the high mobility path in spite of $T_{vc} \ll T_{vv}$ and $T_{cv} \ll T_{cc}$. According to Fig. 3(a), furthermore, we know that $A(\tau) < 0$ and $E(\tau) < 0$ [left panel of Fig. 3(a)] supports the worst condition for conducting the tunneling current, while $A(\tau) > 0$ and $E(\tau) > 0$ [right panel of Fig. 3(a)] the best condition. Eventually, the current flows along one direction from the left side (the low-hole-mass dielectric) to the right side (the low-electron-mass dielectric) in spite of an oscillation of the optical field. This is very much analogous to the carrier transport in the forward bias and reverse bias with respect to the alternating voltage in the semiconductor pn junction [21]. In our study, therefore, it is naturally addressed that the heterojunction in our consideration plays a role of the diode in the petahertz domain, i.e., petahertz diode.

Features of the petahertz diode are nicely demonstrated in Figs. 3(b)–3(e) at a few values of ϕ . Varied profiles of optically induced currents with respect to ϕ confirm that the currents are in fact rectified through the tunneling across the junction. Meanwhile, the transferred charge $P(\tau)$ increases with τ but with piecewise plateaus. The total transferred (tunneling) charge Q_T is calculated by $Q_T = \int_{-\infty}^{\infty} d\tau J_T(\tau)$ [24], which is an almost constant value with respect to ϕ [see Fig. 3(f)], differently from Q of Fig. 1(d).

In Fig. 4, the tunneling currents are compared with respect to the electric field strength E_0 . When E_0 decreases, the current decreases and in addition the rectifying efficiency becomes poor because the displacements of the effective bands are suppressed. In particular, as shown in the inset of Fig. 4, at a fixed value of ϕ , $|Q|$ behaves like E_0^η stably fitted with $\eta = 6 \sim 7$ [25], which implies the non-linear response resulting in the optical-field-induced current in the strong field intensity. However, Q_T does not follow a simple power law, as being understandable from

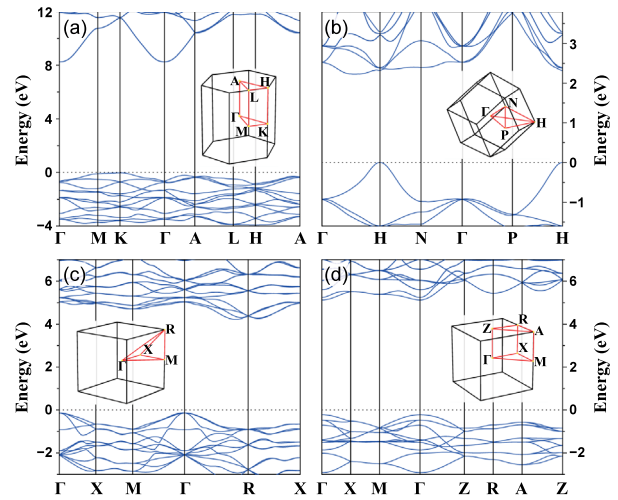


FIG. 5. (a) Electronic structure of a good low-electron-mass dielectric, α -SiO₂ (quartz). (b)–(d) Electronic structures of candidates for the low-hole-mass dielectric: (b) K₂Pb₂O₃, (c) ZrSO, and (d) CaCl₂. Insets show the Brillouin zone and the symmetry directions (red lines).

the rectifying efficiency depending on the field strength. As a matter of fact, $Q_T \times 5000$ in the vanishing field strength is far from $|Q| \times 500$ in the inset.

A natural forthcoming question will be which materials could be possible candidates to realize the proposed junction. First, the low-electron-mass dielectrics are actually common, which are already present in many devices. However, it is rather challenging to look for good low-hole-mass dielectrics. Hautier *et al.* [26] identified the design principles of low-hole-mass oxides and suggested a few possible oxides like PbTiO₃ (tetragonal), B₆O, ZrSO, Tl₄V₂O₇, K₂Pb₂O₃, K₂Sn₂O₃, Pb₂Sn₂O₃, and so on.

Finally, using the density functional theory (DFT) formulation, we calculate and provide the electronic band structures of SiO₂, K₂Pb₂O₃, ZrSO, and CaCl₂ in Fig. 5. In fact, SiO₂, a dielectric used in the principle experiment by Schiffrin *et al.* [13] is a good low-electron-mass dielectric, as shown in Fig. 5(a). On the other hand, in Figs. 5(b)–5(d), we suggest the effective low-hole-mass dielectrics K₂Pb₂O₃, ZrSO, and CaCl₂, whose polarities are implied by their electronic structures. In detailed calculations, the generalized gradient approximation (GGA) by the Perdew-Burke-Ernzerhof (PBE) functional [27] is employed and the Green's function perturbation theory, i.e., the GW approximation [28] is further applied for the computation of SiO₂, K₂Pb₂O₃, and ZrSO.

In summary, in a theoretical investigation of dielectrics under the optical pumping, we have proposed an asymmetric conduction of the optical-field-induced current. For this purpose, a heterojunction has been suggested, which consists of two different dielectrics: one with the low hole mass ($m_h^* \ll m_e^*$) and the other with the low electron mass ($m_e^* \ll m_h^*$). Across the junction, the tunneling current has

been found to asymmetrically flow from the low-hole-mass dielectric to the low-electron-mass one. This finding indicates a new concept of the petahertz diode, probably a key ingredient to advance a realization of the light-wave electronics in the solid state. Finally, we suggested the candidate dielectrics for a proper design of the heterojunction.

This work was supported by the Leading Foreign Research Institute Recruitment Program (Grant No. 2012K1A4A3053565) and the Basic Science Research Program (Grant No. 2013R1A1A2007388) through the National Research Foundation of Korea (NRF) funded by the Ministry of Education, Science and Technology (MEST).

*Corresponding author.
jdlee@dgist.ac.kr

- [1] F. Krausz and M. Ivanov, *Rev. Mod. Phys.* **81**, 163 (2009).
- [2] M. Drescher, M. Hentschel, R. Kienberger, M. Uiberacker, V. Yakovlev, A. Scrinzi, Th. Westerwalbesloh, U. Kleineberg, U. Heinzmann, and F. Krausz, *Nature (London)* **419**, 803 (2002).
- [3] R. Kienberger *et al.*, *Nature (London)* **427**, 817 (2004).
- [4] A. L. Cavalieri *et al.*, *Nature (London)* **449**, 1029 (2007).
- [5] M. Uiberacker *et al.*, *Nature (London)* **446**, 627 (2007).
- [6] M. Schultze *et al.*, *Science* **328**, 1658 (2010).
- [7] E. Goulielmakis *et al.*, *Nature (London)* **466**, 739 (2010).
- [8] K. Klünder *et al.*, *Phys. Rev. Lett.* **106**, 143002 (2011).
- [9] S. Neppl, R. Ernstorfer, E. M. Bothschafter, A. L. Cavalieri, D. Menzel, J. V. Barth, F. Krausz, R. Kienberger, and P. Feulner, *Phys. Rev. Lett.* **109**, 087401 (2012).
- [10] J. D. Lee, *Phys. Rev. B* **86**, 035101 (2012).
- [11] J. D. Lee, *Phys. Rev. Lett.* **111**, 027401 (2013).
- [12] C. Lemell, S. Neppl, G. Wachter, K. Tórkési, R. Ernstorfer, P. Feulner, R. Kienberger, and J. Burgdörfer, *Phys. Rev. B* **91**, 241101(R) (2015).
- [13] A. Schiffrin *et al.*, *Nature (London)* **493**, 70 (2013).
- [14] M. Krüger, M. Schenk, and P. Hommelhoff, *Nature (London)* **475**, 78 (2011).
- [15] G. Wachter, C. Lemell, J. Burgdörfer, M. Schenk, M. Krüger, and P. Hommelhoff, *Phys. Rev. B* **86**, 035402 (2012).
- [16] S. Zerebtsov *et al.*, *Nat. Phys.* **7**, 656 (2011).
- [17] P. G. Hawkins and M. Y. Ivanov, *Phys. Rev. A* **87**, 063842 (2013).
- [18] S. Y. Kruchinin, M. Korbman, and V. S. Yakovlev, *Phys. Rev. B* **87**, 115201 (2013).
- [19] V. Apalkov and M. I. Stockman, *Phys. Rev. B* **86**, 165118 (2012).
- [20] G. Wachter, C. Lemell, J. Burgdörfer, S. A. Sato, X.-M. Tong, and K. Yabana, *Phys. Rev. Lett.* **113**, 087401 (2014).
- [21] S. M. Sze and K. K. Ng, *Physics of Semiconductor Devices*, 3rd ed. (Wiley-Interscience, New York, 2006).
- [22] Conventionally, ϕ is defined such that a peak of the electric field is positioned at $\phi = 0$. In the present study, however, its definition is slightly different.
- [23] G. D. Mahan, *Many-Particle Physics* (Plenum, New York, 1990).
- [24] Transferred charge Q_T may induce the polarization field whose strength would be approximately $Q_T/S\epsilon_0$, where S is the junction cross section and ϵ_0 the permittivity. Therefore, if $E_0 \gg Q_T/S\epsilon_0$, the polarization field will be negligible compared to the applied optical field. Otherwise, the polarization field should be properly handled.
- [25] See Supplemental Material at <http://link.aps.org/supplemental/10.1103/PhysRevLett.116.057401> for a discussion of the effects of multiple bands on the nonlinear excitation and its concomitant tunneling.
- [26] G. Hautier, A. Miglio, G. Ceder, G.-M. Rignanese, and X. Gonze, *Nat. Commun.* **4**, 2292 (2013).
- [27] J. P. Perdew, K. Burke, and M. Ernzerhof, *Phys. Rev. Lett.* **77**, 3865 (1996).
- [28] L. Hedin, *Phys. Rev.* **139**, A796 (1965).